

Bloch-Grüneisen temperature and universal scaling of normalized resistivity in doped graphene revisited

Khoe Van Nguyen^{1,2,3*} and Yia-Chung Chang^{1,4†}

¹ *Research Center for Applied Sciences, Academia Sinica, Taipei 115, Taiwan*

² *Molecular Science and Technology, Taiwan International Graduate Program, Academia Sinica, Taipei 115, Taiwan*

³ *Department of Physics, National Central University, Chungli, 320 Taiwan and*

⁴ *Department of Physics, National Cheng-Kung University, Tainan 701, Taiwan*

(Dated: July 3, 2020)

In this work, we resolved some controversial issues on the Bloch-Grüneisen (BG) temperature in doped graphene via analytical and numerical calculations based on full inelastic electron-acoustic-phonon (EAP) scattering rate and various approximation schemes. Analytic results for BG temperature obtained by semi-elastic (SI) approximation (which gives scattering rates in excellent agreement with the full inelastic scattering rates) are compared with those obtained by quasi-elastic (QE) approximation and the commonly adopted value of $\Theta_F^{LA} = 2\hbar v_{LA} k_F / k_B$. It is found that the commonly adopted BG temperature in graphene (Θ_F^{LA}) is about 5 times larger than the value obtained by the QE approximation and about 2.5 times larger than that by the SI approximation, when using the crossing-point temperature where low-temperature and high-temperature limits of the resistivity meet (criterion 1). The corrected analytic relation based on SI approximation agrees extremely well with the transition temperatures determined by fitting the the low- and high- T behavior of available experimental data of graphene's resistivity. We also introduce a way to determine the BG temperature including the full inelastic EAP scattering rate and the deviation of electron energy from the chemical potential (μ) numerically by finding the maximum of $\partial\rho(\mu, T)/\partial T$ (criterion 2). It is found that the BG temperature determined by the full numerical calculation with criterion 2 falls between the values obtained analytically via the SI approximation with criterion 1 ($\Theta_{BG,1}$) and criterion 2 ($\Theta_{BG,2} \approx 1.35\Theta_{BG,1}$) but neglecting the contribution of electron energies away from μ . Using the analytic expression of $\Theta_{BG,1}$ we can prove that the normalized resistivity defined as $R_1 = \rho(\mu, T)/\rho(\mu, \Theta_{BG,1})$ plotted as a function of $(T/\Theta_{BG,1})$ is independent of the carrier density. Applying our results to the experimental data extracted from [Phys. Rev. Lett. 105, 256805 (2010)] shows a universal scaling behavior, which is different from previous studies.

Bloch-Grüneisen temperature (Θ_{BG}) in doped graphene has been extensively discussed in the literature [1-31]. Θ_{BG} is usually defined as the crossing point in temperature between the low-temperature (LT) limit expression and high-temperature (HT) limit expression for resistivity as functions of temperature [1-10]. Θ_{BG} is an important characteristic temperature for designing graphene-based devices in applications such as optical detectors, bolometers [16, 22] and in cooling pathways and supercollisions [11, 22, 24, 28-31]. If one considers separate contributions in Θ_{BG} due to longitudinal-acoustic (LA) and transverse-acoustic (TA) phonon scatterings, simple analytic expressions for Θ_F^a ($a = LA, TA$) can be obtained based on the LT- and HT-limit expressions for resistivity. The current general consensus is that $k_B\Theta_F^a = 2\hbar v_a k_F$ ($a = LA, TA$) through analyses based on quasi-elastic scattering approximation [1-27]. In the LT limit, it can be shown that $\rho_a^{LT}(\mu, T) \propto T^4$ and in the HT regime $\rho_a^{HT}(\mu, T) \propto T$ [1, 2].

Critical inconsistencies exist in Figs. 2b and 3b of [2] and in Fig. 2 of [10]. The crossing points found in both studies are $\sim 5 - 6$ times smaller than the theoretical

values predicted by Θ_F^{LA} above. To remedy this inconsistency an artificial scaling parameter of $\zeta = 0.2$ was introduced in [2] to make the BG resistivity $\rho(\mu, \zeta\Theta_F^{LA})$ fall within the experimentally accessible range. Using the same definition of Θ_F^a , it was shown that the BG transition occurs for $T < 0.2\Theta_F^{LA}$ [16], $T \lesssim 0.15\Theta_F^a$ [23], $T \lesssim 0.25\Theta_F^a$ [24, 25], and $1/\tau_a^{LT}(\mu, T) \propto T^4$ for $T \lesssim 0.2\Theta_F^a$ as implied in Ref. [15]. Our analysis based on quasi-elastic approximation also gives the same conclusion, i.e. $k_B\Theta_{BG,0} = 2\hbar v_{LA} k_F / 5$. More detailed analyses are given in supplemental material (SM)[32].

Contrary to the above, the analyses in Refs.[28-31] suggest that $k_B\Theta_{BG} = \hbar v_{LA} k_F$. Note that in Ref. [22] $\Theta_{BG} = \Theta_F^{LA} = 2\hbar v_{LA} k_F / k_B$ was used in the arguments and calculations but their results are compared not only with those from Refs. [11-13] using the same Θ_F^{LA} but also with those from Ref. [28] using $\Theta_{BG} = \hbar v_{LA} k_F / k_B$. To resolve these controversies a more careful analysis of the BG temperature and a revisit of the universal scaling of the normalized resistivity $R(T/\Theta_{BG})$ in doped graphene is needed.

The resistivity in doped graphene can be calculated according to [33, 34]

$$\rho^{-1}(\mu, T) = \sigma(\mu, T) = e^2 \int \frac{k dk}{\pi} v_F^2 \tau(\epsilon_k) \left[-\frac{df(\epsilon_k)}{d\epsilon_k} \right], \quad (1)$$

where σ is the conductivity. In common practice, $-df(\epsilon_k)/d\epsilon_k$ is approximated by $\delta(\epsilon_k - \mu)$ since $\tau(\epsilon_k)|_{\epsilon_k}$

* nvkhoe@gate.sinica.edu.tw

† yiachang@gate.sinica.edu.tw

is slow varying over the range of $k_B T$. With this approximation we have [34]

$$\rho_\mu(\mu, T) = \frac{|\mu|}{4e^2 \hbar v_F^3 \rho_m} \int d\theta (1 - \cos \theta) \sum_{a,p} D_a^p(\theta) \operatorname{csch}(\hbar \Omega_a^p / k_B T), \quad (2)$$

where $D_a^p(\theta) \approx B^2 T_a^p(\theta)$ (when E_1 is neglected) and $T_a^p(\theta)$ describes the angular dependence of the net electron-acoustic-phonon (EAP) scattering strength with $a = LA, TA$ and $p = \pm$ for phonon absorption or emission ($T_a^p(\theta)$ is depicted in Fig. 1 of [34]). $\hbar \Omega_a^p$ is the corresponding phonon energy. Throughout the paper, we only consider the n -doped case. Due to electron-hole symmetry in the Dirac Hamiltonian, the behavior of p -doped case will be identical. We use $v_F = 1.0 \times 10^6$ (m/s), $v_{LA} = 2.0 \times 10^4$ (m/s), $v_{TA} = 1.3 \times 10^4$ (m/s), $\rho_m = 7.6 \times 10^{-7}$ (Kg/m²) [34, 35], $g_0 = 20$ (eV) and $\beta = 3$ [14, 34].

Using the quasielastic (QE) approximation for scattering rates [1, 2] and setting $\rho_{QE}^{LT}(\mu, T) = \rho_{QE}^{HT}(\mu, T)$ gives [32]

$$k_B \Theta_{BG,0} = \sqrt[3]{15} \hbar v_{LA} k_F / 2\pi \approx k_B \Theta_F^{LA} / 5, \quad (3)$$

where $\Theta_F^{LA} = 2\hbar v_{LA} k_F / k_B$ is a characteristic temperature, which is often used as the BG temperature in the literature [1-27]. The more appropriate BG temperature within quasielastic approximation should be $\Theta_{BG,0}$, although it is still quite different from the results derived from the full calculation. The transferred acoustic phonon energy is determined by $\hbar \omega_a^p = \hbar v_a q_a^p \approx 2\hbar v_a k \sin(\theta/2)$ since $v_a / v_F \ll 1$ [34]. Thus, we obtain $\langle \hbar \omega_a^p \rangle_p = 2\hbar v_a k_F \sin(\theta/2)$ for $\epsilon_k = \mu$. Therefore, $\max(\langle \hbar \omega_a^p \rangle_p) = 2\hbar v_a k_F = k_B \Theta_F^a$ has the physical meaning of the maximal transferred acoustic phonon energy.

$$k_B \Theta_F^a = 2\hbar v_a k_F. \quad (4)$$

In Refs. [3, 22] it is suggested that $k_B \Theta_{BG}$ is close to the maximum transferred phonon energy.

Next, we consider a semi-inelastic (SI) approximation, which gives results very close to the full inelastic scattering calculation [34]. In the SI approximation, the LT and HT limits of $\tau^{-1}(\mu, T)$ are given by

$$\rho_{SI}^{LT}(\mu, T) = \frac{3v_F (k_B T)^4}{e^2 \rho_m |\mu|^3 \hbar v_{LA}^5} [2E_1^2 + B^2(1 + \beta_v^5)] \quad (5a)$$

and

$$\rho_{SI}^{HT}(\mu, T) = \frac{\pi k_B T}{4e^2 \rho_m v_{LA}^2 \hbar v_F^2} [E_1^2 + 2B^2(1 + \beta_v^2)], \quad (5b)$$

respectively, where $E_1 = g_0 / \epsilon(q)$ is the screened deformation potential for LA phonon, $B = 3\beta\gamma_0/4$ denotes electron-phonon coupling strength due to unscreened gauge fields for both LA and TA phonons, and $\beta_v =$

v_{LA}/v_{TA} with v_{LA} (v_{TA}) being the sound velocity of LA (TA) phonon. Since $E_1^2/B^2 \ll 1$, it is a good approximation to neglect the E_1 contribution.

By setting $\rho_{SI}^{LT}(\mu, T) = \rho_{SI}^{HT}(\mu, T)$ we obtain [32]

$$\Theta_{BG,1} = \sqrt[3]{\frac{2E_1^2 \Theta_{d,1}^3 + B^2 (\Theta_{LA,1}^3 + \beta_v^5 \Theta_{TA,1}^3)}{2E_1^2 + B^2(1 + \beta_v^5)}}, \quad (6a)$$

$$\approx \sqrt[3]{\frac{\Theta_{LA,1}^3 + \beta_v^5 \Theta_{TA,1}^3}{1 + \beta_v^5}} = \sum_a b_a \hbar v_a k_F / k_B \quad (6b)$$

where

$$k_B \Theta_{d,1} = \sqrt[3]{\pi/24} \hbar v_{LA} k_F \approx \hbar v_{LA} k_F / 2 \quad (6c)$$

and

$$k_B \Theta_{a,1} = \sqrt[3]{\pi/6} \hbar v_a k_F \approx 4\hbar v_a k_F / 5 \quad (6d)$$

($a = LA, TA$) denote separate contributions from deformation potential (labeled by d) and unscreened LA and TA phonon scatterings. And $b_a = \sqrt[3]{\pi/6} (\delta_{a,LA} + \beta_v \delta_{a,TA}) \sqrt[3]{\frac{1 + \beta_v^2}{1 + \beta_v^5}}$.

Because the resistivity $\rho_\mu(\mu, T)$ is proportional to T^4 (T) in the low- T (high- T) limit, Θ_{BG} should be near the maximum of $\partial \rho_\mu(\mu, T) / \partial T$. Using the semi-inelastic scattering rate at $\epsilon_k = \mu$, we have [34]

$$\rho_\mu(\mu, T) = \frac{3v_F (k_B T)^4}{e^2 \rho_m \hbar |\mu|^3} \left\{ \frac{1}{v_{LA}^5} \left[\frac{2E_1^2}{1 + c_1 \alpha_{LA}^3} + \frac{B^2}{1 + c_0 \alpha_{LA}^3} \right] + \frac{1}{v_{TA}^5} \frac{B^2}{1 + c_0 \alpha_{TA}^3} \right\}$$

$$\approx \frac{\hbar \Lambda (k_B T)^4}{e^2 |\mu|^3} \sum_a \frac{\delta_{a,LA} + \beta_v^5 \delta_{a,TA}}{1 + c_0 \alpha_a^3} \quad (7)$$

where $\Lambda = \frac{3v_F B^2}{\rho_m \hbar^2 v_{LA}^5}$, $c_0 = 16.5$, $c_1 = 65.7$, and $\alpha_a = T / \Theta_F^a$ [34].

Using Eq. (7) we can solve the equation

$$\partial^2 \rho_\mu(\mu, T) / \partial T^2 = 0 \quad (8)$$

analytically and get the BG temperature at the peak of $\partial \rho_\mu(T) / \partial T$ (See Sec. III in SM [32] for derivations)

$$\Theta_{BG,2} \approx \sqrt[3]{\frac{\Theta_{LA,2}^3 + \beta_v^5 \Theta_{TA,2}^3}{1 + \beta_v^2}} = \tilde{b}_a \hbar v_a k_F / k_B, \quad (9a)$$

where

$$k_B \Theta_{a,2} = \sqrt[3]{16/c_0} \hbar v_a k_F \quad (9b)$$

with $\tilde{b}_a = (\delta_{a,LA} + \beta_v \delta_{a,TA}) \sqrt[3]{\frac{3(1 + \beta_v^{-1})}{c_0(1 + \beta_v^2)}}$. Note that the E_1 term has been neglected in Eq. (9a). We found

$$\Theta_{BG,1} / \Theta_{BG,2} = b_a / \tilde{b}_a \approx 0.728. \quad (10)$$

The theoretical results described by Eqs. (3), (4), (6), and (9) are plotted in Fig. 1 for comparison.

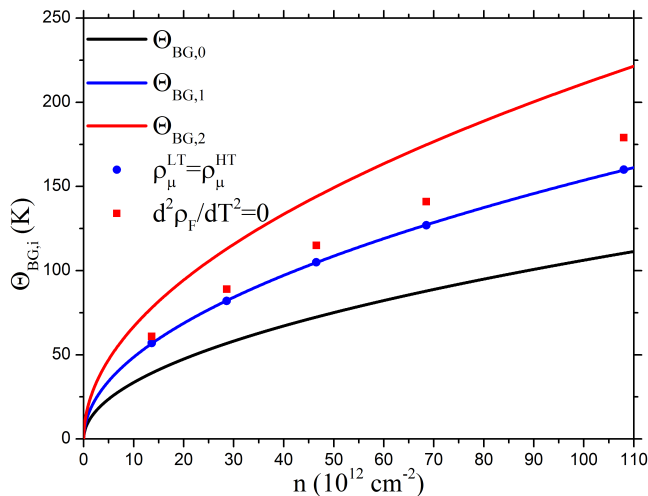


FIG. 1. BG temperatures $\Theta_{BG,i}$ determined by three different ways with solid black, blue, and red curves for $i = 0, 1$, and 2, respectively. Blue circles display $\Theta_{BG,1}$ inferred from fitting LT and HT limits of experimental data of [2] at five densities ranging from $13.6 - 108 \times 10^{12} \text{ cm}^{-2}$ by using scattering rates for $\epsilon_k = \mu$ with semi-inelastic approximation. The red squares are obtained by taking derivatives of the resistivity including contributions from all ϵ_k 's with full inelastic scattering rates.

Above we have shown that for the special case of $\epsilon_k = \mu$, $\Theta_{BG,1}$ and $\Theta_{BG,2}$ obtained by two different approaches can differ by about 30%. For full considerations including contribution from all possible ϵ_k 's, it is impossible to determine the temperature dependence of resistivity analytically. However, it is possible to calculate $\rho(\mu, T)$ according to Eq. (1) numerically with the full inelastic scattering rate without fixing ϵ_k at μ . We then take the derivatives of the full $\rho(\mu, T)$ to determine Θ_{BG} . The results are displayed by the red squares in Fig. 1 at five densities ranging from $13.6 - 108 \times 10^{12} \text{ cm}^{-2}$ corresponding to samples studied in [2] and we see that Θ_{BG} so determined falls between $\Theta_{BG,1}$ and $\Theta_{BG,2}$.

To compare with experimental results, we extract the experimental data of resistivities in n-doped graphene from [2] at five carrier densities and plot them as colored dots in Fig. 2 for $n = 13.6 \times 10^{12} \text{ cm}^{-2}$ (black), $28.6 \times 10^{12} \text{ cm}^{-2}$ (red), $46.5 \times 10^{12} \text{ cm}^{-2}$ (green), $68.5 \times 10^{12} \text{ cm}^{-2}$ (blue), and $108 \times 10^{12} \text{ cm}^{-2}$ (magenta). We can fit these data well by using Eq. (1) with the full inelastic scattering rates as solid curves in Fig. 2 which essentially go through the data points with slight deviation at the high-temperature end. To fit the data, a residual scattering rate beyond the acoustic phonon scattering mechanisms is added for a given n ; that is, $1/\tau_0 = 9.4, 7.9, 6.6, 5.95$, and 5.5 THz for the five respective carrier densities. The values of other constants adopted (E_1, B, β_v) are the same as those used in [34]. We can also fit these data at high- and low- T limits by using Eq. (5) with semi-inelastic scattering rates as shown in dash-dotted and dashed curves, respectively. The cross-

ing points between those curves determine $\Theta_{BG,1}$, which are shown as blue circles in Fig. 1 and they fall perfectly on the theoretical curve (blue solid). For comparison, $\Theta_{BG,0}$ determined by using the low- and high- T quasielastic scattering rates [1, 2] as given in Eq. (3) as a function of density is shown as the black solid curve.

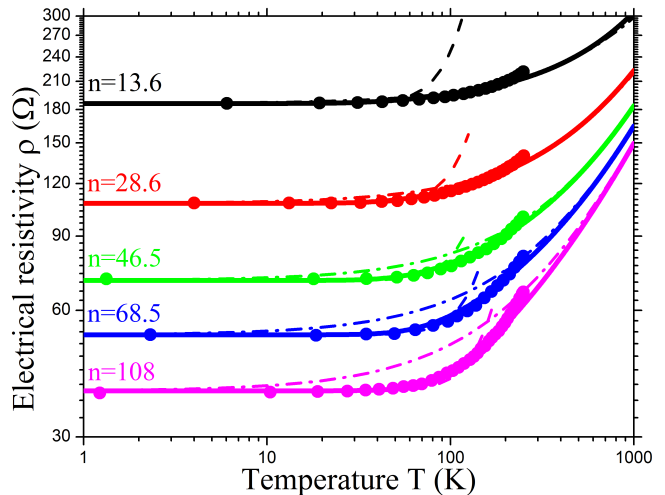


FIG. 2. Log-log plot of the electrical resistivity of graphene/SiO₂ with $n = 13.6 \times 10^{12} \text{ cm}^{-2}$ (in black), $28.6 \times 10^{12} \text{ cm}^{-2}$ (in red), $46.5 \times 10^{12} \text{ cm}^{-2}$ (in green), $68.5 \times 10^{12} \text{ cm}^{-2}$ (in blue), and $108 \times 10^{12} \text{ cm}^{-2}$ (in magenta) as a function of T . The solid curves are $\rho_F(n, T)$ obtained by Eq. (1) with suitable parameters. The dashed-dotted and dashed curves respectively demonstrate the fitted high- T and low- T resistivities by using $\rho_{SI}^{HT}(\mu, T)$ and $\rho_{SI}^{LT}(\mu, T)$ given by Eq. (5). The experimental data shown by colored circles are extracted from [2].

The total doping-dependent Bloch-Grüneisen temperatures Θ_{BG} (shown by the red squares in Fig. 1 at five densities) are determined from the peak values of $\partial\rho_F(n, T)/\partial T$ plotted in Fig. 3. Note that, $\rho_F(n, T)$ are obtained by using the full calculation described in Eq. (1) with the inelastic scattering rate plus a correction term $1/\tau_0$ which takes into account scattering mechanisms beyond the acoustic-phonon scattering. For comparison, we also show $\partial\rho_\mu(n, T)/\partial T$ as dash-dotted curves in Fig. 3. It should be noted that adding a constant correction term $1/\tau_0$ to the scattering rate will have no effect on $\partial\rho_\mu(n, T)/\partial T$. For a given n , $\Theta_{BG,2}$ shifts to the right of Θ_{BG} since the ratio of $\rho_\mu(n, T)$ to full $\rho(n, T)$ falls between 0.7 and 1[34]. This comes from the fact that $-df(\epsilon)/d\epsilon$ can be approximated by $\delta(\epsilon - \mu)$ to obtain $\rho_\mu(n, T)$ only when $|\epsilon|\tau(\epsilon_k)$ is slow varying over $k_B T$, which is not quite satisfied in graphene [34].

Finally, we consider the universal scaling of normalized resistivity by using the well justified SI approximation and the full inelastic scattering rate for $\epsilon_k = \mu$. The normalized resistivity is defined as[36]

$$R_i(T/\Theta_{BG,i}) = \rho(\mu, T)/\rho(\mu, \Theta_{BG,i}). \quad (11)$$

In the SI approximation, $\rho(\mu, T)$ is given by Eq. (7) and

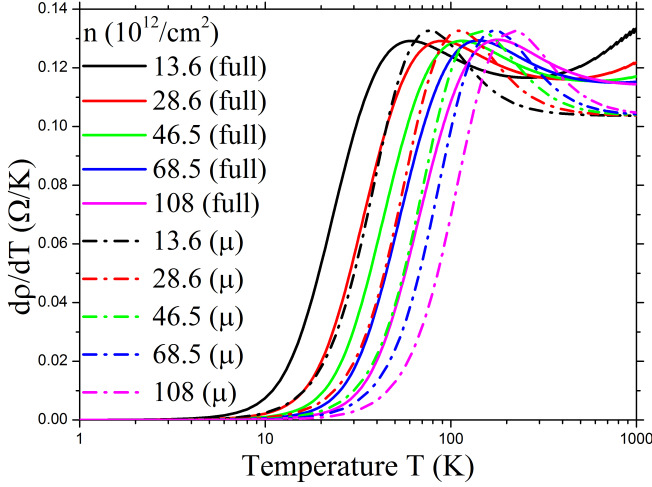


FIG. 3. Derivative of net resistivity, $\partial\rho_F(n, T)/\partial T$ (which includes a constant correction term in scattering rate due to mechanisms beyond EAP scattering) as a function of T . Solid curves are from numerical calculation based on full inelastic scattering rate. For comparison, we also show $\partial\rho_\mu(n, T)/\partial T$ due to semi-inelastic scattering rate $\tau_{SI}^{-1}(\mu, T)$ (dashed-dotted curves)[34].

we have

$$R_i \left(\frac{T}{\Theta_{BG,i}} \right) = \left(\frac{T}{\Theta_{BG,i}} \right)^4 \frac{\sum_a \frac{\delta_{a,LA} + \beta_v^5 \delta_{a,TA}}{1 + c_0 \alpha_{a,i}^3}}{\sum_a \frac{\delta_{a,LA} + \beta_v^5 \delta_{a,TA}}{1 + c_0 \alpha_{a,i}^3}}, \quad (12)$$

where $\alpha_{a,i} = \Theta_{BG,i}/\Theta_F^a$ with $i = 1, 2$.

From Eq. (5), we see that $\rho_{SI}^{LT}(\mu, \Theta_{BG,i}) \propto \frac{(k_B \Theta_{BG,i})^4}{|\mu|^3} \propto |\mu|$ and similarly $\rho_{SI}^{HT}(\mu, \Theta_{BG,i}) \propto (k_B \Theta_{BG,i}) \propto |\mu|$. Therefore, the normalized resistivity of doped graphene is independent of $|\mu|$ and that is why one can get a universal curve for $R_i(T/\Theta_{BG,i})$ regardless of doping level of the sample. This feature comes out naturally from our approach by using the semi-inelastic scattering rate. The normalized resistivity R_i is proportional to $(T/\Theta_{BG,i})^4$ in the LT limit and $T/\Theta_{BG,i}$ in the HT limit.

Now instead of the SI approximation, we use the resistivity given in Eq.(2) with full inelastic scattering rate

$$R^{in} = \frac{\int d\theta \sin^2 \frac{\theta}{2} \sum_{a,p} \frac{T_a^p(\theta)}{v_a} \text{csch}\left(\frac{Q_a^p(\theta)\Theta_F^a}{2T}\right)}{\int d\theta \sin^2 \frac{\theta}{2} \sum_{a,p} \frac{T_a^p(\theta)}{v_a} \text{csch}\left(\frac{Q_a^p(\theta)\Theta_F^a}{2\Theta_{BG,i}}\right)}, \quad (13)$$

where $Q_a^p(\theta) = q_a^p/k$ is the ratio of the phonon momentum to electron momentum[34]. Our numerical results indicate that R^{in} is almost identical to R_1 and R_2 . Obviously, as $T \rightarrow \Theta_{BG,i}$, R_i and R^{in} should approach 1.

The results for R_1 together with the results taken from Ref. [2] are demonstrated in Fig. 4. We found a significant difference between our results and those from [2], especially for $T/\Theta_{BG,i} < 1$. It is noted that in Ref. [2]

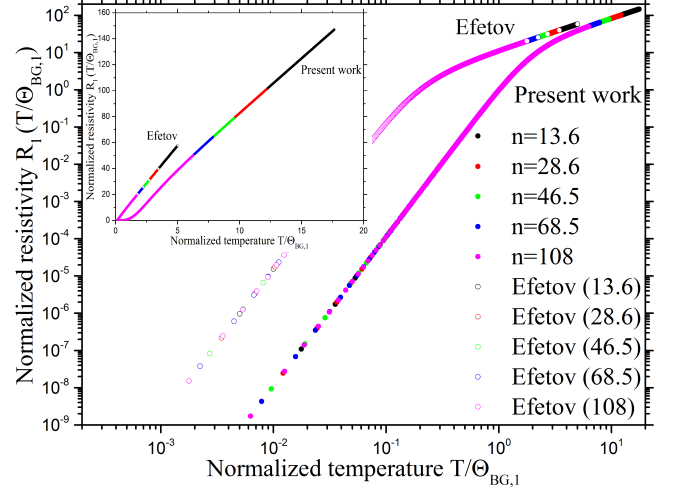


FIG. 4. Log-log plot of normalized resistivity $R_1(T/\Theta_{BG,1})$ as a function of $T/\Theta_{BG,1}$ for various carrier densities ($n = 13.6 - 108 \times 10^{12} \text{ cm}^{-2}$). The results of Ref. [2] are also reproduced for comparison. The inset shows the corresponding linear plot of R_1 . For ease of observing the universal behaviors, $T_{max} = 1000 \text{ K}$ is used.

the normalized resistivity is defined as $R_0 \left(\frac{T}{\Theta_{BG}} \right) = \rho(\mu, T)/\rho(\mu, \xi\Theta_{BG})$ with $\xi = 0.2$ instead of 1. Since Θ_{BG} adopted in Ref. [2] is $2\hbar v_{LA} k_F/k_B = \Theta_F^{LA}$, which makes $0.2\Theta_F^{LA} \approx \Theta_{BG,0}$, the BG temperature determined by QE approximation given in Eq. (3). Although the universal scaling or behavior of R_i as a function of the normalized temperature $T/\Theta_{BG,i}$ does not depend on μ , for the same T range of investigation, the heavier graphene gets doped (i.e. the larger $|\mu|$ induces the larger $\Theta_{BG,i}$), the narrower the range of $T/\Theta_{BG,i}$ becomes.

In conclusion, we have clarified the issues of BG temperatures in graphene via analytical and numerical calculations based on full inelastic EAP scattering rate and various approximation schemes. We found that the commonly adopted BG temperatures in graphene ($k_B \Theta_F^{LA} = 2\hbar v_{LA} k_F$) [1–27] need to be corrected by a factor around 2.5, when using the same criterium [$\rho_\mu^{LT}(\mu, T) = \rho_\mu^{HT}(\mu, T)$]. The BG temperature induced by the in-plane EAP scattering in semi-inelastic approximation is uncovered as $\Theta_{BG,1} \approx [(\Theta_{LA,1}^3 + \beta_v^5 \Theta_{TA,1}^3)/(1 + \beta_v^5)]^{1/3}$ with $\Theta_{a,1} = (\pi/6)^{1/3} \hbar v_a k_F/k_B$. The corrected analytic relation agrees extremely well with the transition temperatures determined by fitting the the low- and high- T behavior of available experimental data of graphene's resistivity [2]. We also show that Refs. [15, 16, 23–25] well agree with the quasi-elastic (QE) prediction. When the inelastic EAP scattering rate and the deviation of electron energy from the chemical potential (μ) are fully taken into account, the resistivity $\rho(\mu, T)$ can only be described numerically. For this case we determine the BG temperature by the point where $\partial\rho(\mu, T)/\partial T$ is a maximum and thus $\partial^2\rho(\mu, T)/\partial T^2 = 0$ (criterion 2). If we also apply criterium 2 to find the BG tempera-

ture in the SI approximation, we get $\Theta_{BG,2} \approx [(\Theta_{LA,2}^3 + \beta_v^2 \Theta_{TA,2}^3)/(1 + \beta_v^2)]^{1/3}$ with $k_B \Theta_{a,2} = (16/c_0)^{1/3} \hbar v_a k_F$, which happen to be very close to the value $\hbar v_a k_F$ deduced in Refs. [28–31]. We found that the BG temperature determined by the full numerical calculation with criterium 2 falls between the values obtained via the SI approximation with criterium 1 ($\Theta_{BG,1}$) and criterium 2 ($\Theta_{BG,2} \approx 1.35 \Theta_{BG,1}$). These values are about a factor 2 higher than the BG temperature ($\Theta_{BG,0}$) obtained with the oversimplified QE approximation and a factor 2-2.5 lower than the commonly adopted value of Θ_F^{LA} .

Finally, the resistivity normalized to its value at $T =$

$\Theta_{BG,i}$ [$R_i = \rho(\mu, T)/\rho(\mu, \Theta_{BG,i})$] plotted as a function of the normalized temperature $T/\Theta_{BG,i}$ displays a universal scaling behavior, which is independent of the carrier density[2]. Applying our results to the experimental data extracted from Ref. [2] does show such a universal scaling behavior, which obeys the relation $R_i(1) = 1$.

ACKNOWLEDGMENTS

Work supported in part by Ministry of Science and Technology (MOST), Taiwan under contract nos. 107-2112-M-001-032 and 108-2112-M-001-041.

-
- [1] E. H. Hwang and S. D. Sarma, Phys. Rev. B 77, 115449 (2008).
- [2] D. K. Efetov and P. Kim, Phys. Rev. Lett. 105, 256805 (2010).
- [3] M. S. Fuhrer, Physics 3, 106 (2010).
- [4] H. Min, E. H. Hwang, and S. Das Sarma, Phys. Rev. B 83, 161404(R) (2011).
- [5] S. Das Sarma, S. Adam, E. H. Hwang, E. Rossy, Rev. Mod. Phys. 83, 407 (2011).
- [6] D. R. Cooper, B. D’Anjou, N. Ghattamaneni, B. Harack, M. Hilke, A. Horth, N. Majlis, M. Massicotte, L. Vandersburger, E. Whiteway and V. Yu, ISRN Condens. Matter Phys. 2012, 1 (2012).
- [7] C.-H. Park, N. Bonini, T. Sohier, G. Samsonidze, B. Kozinsky, M. Calandra, F. Mauri, and N. Marzari, Nano Lett. 14, 1113 (2014).
- [8] V. Meunier, A. G. Souza Filho, E. B. Barros, M. S. Dresselhaus, Rev. Mod. Phys. 88, 025005 (2016).
- [9] L. Rani and N. Singh, J. Phys.: Condens. Matter 29, 255602 (2017).
- [10] R. D’Souza and S. Mukherjee, Phys. Rev. B 95, 085435 (2017).
- [11] R. Bistritzer and A. H. MacDonald, Phys. Rev. Lett. 102, 206410 (2009).
- [12] S. S. Kubakaddi, Phys. Rev. B 79, 075417 (2009).
- [13] J. K. Viljas and T. T. Heikkila, Phys. Rev. B 81, 245404 (2010).
- [14] E. V. Castro, H. Ochoa, M. I. Katsnelson, R. Gorbachev, D. C. Elias, K. S. Novoselov, A. K. Geim, and F. Guinea, Phys. Rev. Lett. 105, 266601 (2010).
- [15] E. Mariani and Felix von Oppen, Phys. Rev. B 82, 195403 (2010).
- [16] J. Yan, M.-H. Kim, J. A. Elle, A. B. Sushkov, G. S. Jenkins, H. M. Milchberg, M. S. Fuhrer and H. D. Drew, Nature Nanotechnol. 7, 472 (2012).
- [17] W. Chen and Aashish A. Clerk, Phys. Rev. B 86, 125443 (2012).
- [18] E. Munoz, J. Phys.: Condens. Matter 24, 195302 (2012).
- [19] K. C. Fong and K. C. Schwab, Phys. Rev. X 2, 031006 (2012).
- [20] R. Somphonsane, H. Ramamoorthy, G. Bohra, G. He, D. K. Ferry, Y. Ochiai, N. Aoki, and J. P. Bird, Nano Lett. 13, 4305 (2013).
- [21] K. C. Fong, E. E. Wollman, H. Ravi, W. Chen, A. A. Clerk, M. D. Shaw, H. G. Leduc, and K. C. Schwab, Phys. Rev. X 3, 041008 (2013).
- [22] A. C. Betz, S. H. Jhang, E. Pallicchi, R. Ferreira, G. Feve, J.-M. Berroir, and B. Placais, Nature Physics 9, 109 (2013).
- [23] T. Sohier, M. Calandra, C.-H. Park, N. Bonini, N. Marzari, and F. Mauri, Phys. Rev. B 90, 125414 (2014).
- [24] C. B. McKitterick, D. E. Prober, M. J. Rooks, Phys. Rev. B 93, 075410 (2016).
- [25] M. Ansari and S. S. Z. Ashraf, J. Appl. Phys. 122, 164302 (2017).
- [26] T. Gunst, K. Kaasbjerg, and M. Brandbyge, Phys. Rev. Lett. 118, 046601 (2017).
- [27] M. Ansari and S. S. Z. Ashraf, J. Phys.: Condens. Matter 30, 485501 (2018).
- [28] J. C. W. Song, M. Y. Reizer, and L. S. Levitov, Phys. Rev. Lett. 109, 106602 (2012).
- [29] Q. Ma, N. M. Gabor, T. I. Andersen, N. L. Nair, K. Watanabe, T. Taniguchi, and P. Jarillo-Herrero, Phys. Rev. Lett. 112, 247401 (2014).
- [30] K. S. Tikhonov, I. V. Gornyi, V. Yu. Kachorovskii, and A. D. Mirlin, Phys. Rev. B 97, 085415 (2018).
- [31] J. F. Kong, L. Levitov, D. Halbertal and E. Zeldov, Phys. Rev. B 97, 245416 (2018).
- [32] The supplemental material at <http://link.aps.org/supplemental/xxxx>.
- [33] N. W. Ashcroft and N. D. Mermin, Solid State Physics (Saunders, 1976).
- [34] K. V. Nguyen and Y. C. Chang, Phys. Chem. Chem. Phys. 22, 3999 (2020).
- [35] P. Kumaravadivel, M. T. Greenaway, D. Perello, A. Berdyugin, J. Birkbeck, J. Wengraf, S. Liu, J. H. Edgar, A. K. Geim, L. Eaves, and R. K. Kumar, Nat. Commun. 10, 3334 (2019).
- [36] J. M. Ziman, Electrons and Phonons: The Theory of Transport Phenomena in Solids (Oxford University Press, 1960).

Supplemental material of
”Bloch-Grüneisen temperature and universal scaling of
normalized resistivity in doped graphene revisited”

Khoe Van Nguyen^{1,2,3*} and Yia-Chung Chang^{1,4†}

¹ *Research Center for Applied Sciences,
Academia Sinica, Taipei 115, Taiwan*

² *Molecular Science and Technology,
Taiwan International Graduate Program,
Academia Sinica, Taipei 115, Taiwan*

³ *Department of Physics, National Central University, Chungli, 320 Taiwan and*

⁴ *Department of Physics, National Cheng-Kung University, Tainan 701, Taiwan*

(Dated: July 3, 2020)

Abstract

In this supplemental material, we give a more detailed review of current issues related to the Bloch-Grüneisen temperature and provide detailed derivations of all expressions discussed in the main text.

* nvkhoe@gate.sinica.edu.tw

† yiachang@gate.sinica.edu.tw

I. AN OVERVIEW OF CURRENT ISSUES RELATED TO DOPING-DEPENDENT BLOCH-GRÜNEISEN TEMPERATURES IN GRAPHENE

Finite-temperature (T) vibrations of constituent components in a crystal lattice produce quasiparticles named phonons – quantum states of lattice vibrations, which in turn scatter off conducting charged carriers in the lattice causing electrical resistivity ρ [1]. Quantum mechanically, the momentum and energy conservation laws must be fulfilled in these quantum processes [1]. In general, typical three-dimensional (3D) metals have large Fermi surfaces, reasonable Debye temperatures Θ_D 's (i.e. transition temperatures between the high- and low- T regimes of electron-phonon scatterings), and $\rho(T \gg \Theta_D) \propto T/\Theta_D$ and $\rho(T \ll \Theta_D) \propto (T/\Theta_D)^5$ [1–3]. Unlike conventional 3D metals [4], graphene is a two-dimensional (2D) semimetal with zero bandgap, whose low-energy quasiparticles are described by a Dirac-like Hamiltonian with $\epsilon_k = \pm \hbar v_F k$ (+ for n and – for p-type). Thus, the Fermi surface of doped graphene is a small circle, which shrinks into a point in the intrinsic (undoped) limit. Moreover, since graphene has very strong in-plane sp^2 bondings resulting in an unusually high Debye temperature ($\Theta_D > 2000$ K) [5], new characteristic temperatures called Bloch-Grüneisen (BG) temperatures $\Theta_{BG} \ll \Theta_D$ emerge. These new characteristic temperatures were also investigated in the low- T transport of 2D parabolic systems in doped GaAs-Al_xGa_{1-x}As [6] and GaAs-AlGaAs [7] heterostructures.

In 2008, Hwang *et al.* [8] proposed a deformation-potential model, in which longitudinal acoustic (LA) phonons are assumed to dominate graphene's resistivity, and defined the BG temperature in doped graphene as $k_B \Theta_{LA} = 2 \hbar v_{LA} k_F$. Two years later, Efetov *et al.* [9] reported that they had determined $k_B \Theta_{LA} = 2 \hbar v_{LA} k_F$ experimentally by using the quasi-elastic scattering rates with T and T^4 dependences in the high- and low- T limits, respectively to fit their experimental data of graphene's resistivity at ultrahigh carrier densities.

However, recent theoretical and experimental works [10–16] have shown that, in sharp contrast to Refs. [8, 9], transverse acoustic (TA) phonons contribute ~ 2 times greater than LA phonons. The new model is comprised of the screened deformation potential for LA phonons, which only give a tiny contribution, while the unscreened acoustic gauge fields for both LA and TA phonons give dominating contributions.

Therefore, there have so far existed some controversies in the literature regarding the BG temperature in graphene.

II. DETERMINING BLOCH-GRÜNEISEN TEMPERATURES BY SETTING

$$\rho^{LT}(\mu) = \rho^{HT}(\mu)$$

From the electrical conductivity of n-doped graphene with $\epsilon_k = \mu$ at finite μ and T , $\sigma_\mu(\mu, T) = \frac{e^2}{\pi\hbar^2} |\mu| \tau(\mu, T)$, the electrical resistivity is calculated by $\rho_\mu(\mu, T) = \sigma_\mu(\mu, T)^{-1} = \frac{\pi\hbar^2}{e^2 |\mu|} \tau^{-1}(\mu, T)$. In the quasielastic (QE) approximation (i.e. $\frac{1-f(\epsilon')}{1-f(\epsilon)} = 1$) as adopted in References [8, 9], the high-temperature (HT) and low-temperature (LT) quasielastic scattering rates are given by

$$\frac{1}{\tau_{QE}^{HT}} = \frac{1}{\hbar^3} \frac{|\mu|}{4v_F^2} \frac{J_a^2}{\rho_m v_{LA}^2} k_B T, \quad (S1)$$

$$\frac{1}{\langle \tau_{QE}^{LT} \rangle} \approx \frac{1}{\pi} \frac{1}{|\mu|} \frac{1}{k_F} \frac{J_a^2}{2\rho_m v_{LA}} \frac{4!\zeta(4)}{(\hbar v_{LA})^4} (k_B T)^4. \quad (S2)$$

Setting $\frac{1}{\tau_{QE}^{HT}} = \frac{1}{\langle \tau_{QE}^{LT} \rangle}$ (i.e. $\rho_{QE}^{HT} = \rho_{QE}^{LT}$) leads to

$$\frac{4!\zeta(4)}{\pi} \frac{v_F}{v_{LA}^3 \mu^2} (k_B \Theta_{BG,0})^3 = \frac{1}{2} \frac{|\mu|}{v_F^2}, \quad (S3)$$

which gives $(k_B \Theta_{BG,0})^3 = \frac{\pi}{4!2\zeta(4)} (\hbar v_{LA} k_F)^3 = \frac{15}{8\pi^3} (\hbar v_{LA} k_F)^3$, where we have used $\zeta(4) = \pi^4/90$. Thus, we obtain

$$k_B \Theta_{BG,0} = \frac{\sqrt[3]{15}}{2\pi} \hbar v_{LA} k_F \approx 0.4 \hbar v_{LA} k_F = \frac{k_B \Theta_F^{LA}}{5}, \quad (S4)$$

where $\Theta_F^{LA} = 2\hbar v_{LA} k_F$ is a characteristic temperature, which is often interpreted as the Bloch-Grüneisen temperature in the literature [8–11].

Using the semi-inelastic scattering rates at HT and LT limits as discussed in [16],

$$\frac{1}{\tau_{SI}^{HT}(\mu, T)} = \frac{|\mu| k_B T}{4\rho_m v_{LA}^2 \hbar^3 v_F^2} [E_1^2 + 2B^2(1 + \beta_v^2)], \quad (S5)$$

$$\frac{1}{\tau_{SI}^{LT}(\mu, T)} = \frac{3v_F (k_B T)^4}{\pi \rho_m \mu^2 \hbar^3 v_{LA}^5} [2E_1^2 + B^2(1 + \beta_v^5)], \quad (S6)$$

we get

$$E_1^2 + 2B^2(1 + \beta_v^2) = \frac{12T^3}{\pi (\hbar v_{LA} k_F)^3} [2E_1^2 + B^2(1 + \beta_v^5)], \quad (S7)$$

at $T = \Theta_{BG,1}$, from which we obtain

$$k_B \Theta_{BG,1} = \sqrt[3]{\frac{\pi}{12} \frac{E_1^2 + 2B^2(1 + \beta_v^2)}{2E_1^2 + B^2(1 + \beta_v^5)}} \hbar v_{LA} k_F \quad (S8)$$

$$= \sqrt[3]{\frac{2E_1^2 (k_B \Theta_{d,1})^3 + B^2 [(k_B \Theta_{LA,1})^3 + \beta_v^5 (k_B \Theta_{TA,1})^3]}{2E_1^2 + B^2(1 + \beta_v^5)}}, \quad (S9)$$

where

$$k_B \Theta_{d,1} = \sqrt[3]{\frac{\pi}{24}} \hbar v_{LA} k_F,$$

and

$$k_B \Theta_{a,1} = \sqrt[3]{\frac{\pi}{6}} \hbar v_a k_F \quad (a = LA, TA)$$

are separate contributions to the BG temperature due to the negligibly screened deformation potential E_1 and the unscreened acoustic gauge field for LA and TA phonons. $\beta_v = v_{LA}/v_{TA} \approx 1.54$ [14, 17].

Since $E_1(q) = \frac{g_0}{\epsilon(q)}$ with $\epsilon(q) = \epsilon_r + \frac{g_s g_v e^2}{\hbar v_F} \frac{k_F}{q}$ and $B = \frac{3\beta\gamma_0}{4}$ with $\gamma_0 = \frac{2\hbar v_F}{\sqrt{3}a_0}$ and $a_0 = \sqrt{3}a = 0.246$ nm [16], $E_1^2/B^2 \approx 0.09$, and $E_1^2/[2B^2(1 + \beta_v^2)] \approx 0.013 \ll 1$ we can neglect the E_1 term and get

$$k_B \Theta_{BG,1} \approx \sqrt[3]{\frac{\pi}{6} \frac{1 + \beta_v^2}{1 + \beta_v^5}} \hbar v_{LA} k_F \quad (\text{S10})$$

$$= \sqrt[3]{\frac{(k_B \Theta_{LA,1})^3 + \beta_v^5 (k_B \Theta_{TA,1})^3}{1 + \beta_v^5}}. \quad (\text{S11})$$

III. DETERMINING BLOCH-GRÜNEISEN TEMPERATURES BY FINDING THE MAXIMUM OF $\partial\rho(\mu, T)/\partial T$

The scattering rate for $\epsilon_k = \mu$ as a function of μ and T can be well described by an analytic expression based on SI approximation[16]

$$\frac{1}{\tau(\mu, T)} = 12\Upsilon(\mu) \frac{(v_F k_B T)^4}{\mu^4} \left\{ \frac{1}{v_{LA}^5} \left[\frac{2E_1^2}{1 + c_1 \alpha_{LA}^3} + \frac{B^2}{1 + c_0 \alpha_{LA}^3} \right] + \frac{1}{v_{TA}^5} \frac{B^2}{1 + c_0 \alpha_{TA}^3} \right\}, \quad (\text{S12})$$

where $\Upsilon(\mu) = \mu^2/4\pi\rho_m\hbar^3v_F^3$, $c_0 = 16.5$, $c_1 = 65.7$, and $\alpha_a = T/\Theta_F^a$ with $k_B\Theta_F^a = 2\hbar v_a k_F$ ($a = LA, TA$). The electrical resistivity in graphene can be approximately written as

$$\begin{aligned} \rho_\mu(\mu, T) &= \frac{1}{\sigma_\mu(\mu, T)} = \frac{\pi\hbar^2}{e^2|\mu|} \frac{1}{\tau(\mu, T)} \\ &= AY^4 \left\{ \frac{2E_1^2}{b_d + c_d Y^3} + \sum_{a=LA,TA} \frac{B^2}{d_a + c_a Y^3} \right\}, \end{aligned} \quad (\text{S13})$$

where $Y = k_B T$, $A = \frac{24v_F}{e^2\hbar\rho_m}$, $b_d = 8|\mu|^3v_{LA}^5$, $c_d = c_1v_F^3v_{LA}^2$, $d_a = 2|\mu|^3v_a^5$, and $c_a = c_0v_F^3v_a^2$.

Taking the second derivative of $\rho_\mu(\mu, T)$ with respect to T , we get

$$\frac{\partial^2 \rho_\mu(T)}{\partial Y^2} = 6AY^2 \left\{ \frac{2E_1^2 b_d (2b_d - c_d Y^3)}{(b_d + c_d Y^3)^3} + \sum_{a=LA,TA} \frac{B^2 d_a (2d_a - c_a Y^3)}{(d_a + c_a Y^3)^3} \right\}, \quad (\text{S14})$$

Thus, the BG temperature is a solution of the equation $d^2\rho_\mu(\mu, T)/dY^2 = 0$, which we call $\Theta_{BG,2}$. By omitting the screened deformation potential E_1 (which contributes to only about 1%) and setting $X \equiv Y^3$, we are left with a solvable quartic equation with respect to X ,

$$\begin{aligned} \sum_{a=LA,TA} \frac{B^2 b_a (2d_a - c_a Y^3)}{(d_a + c_a Y^3)^3} &= 0 \\ \Leftrightarrow aX^4 + bX^3 + cX^2 + dX + e &= 0, \end{aligned} \quad (\text{S15})$$

where

$$a = -(\beta_v + 1)c_{TA}^4, \quad (\text{S16})$$

$$b = (2\beta_v^4 - 3\beta_v^3 - 3\beta_v + 2)d_{TA}c_{TA}^3, \quad (\text{S17})$$

$$c = (-3\beta_v^6 + 6\beta_v^4 + 6\beta_v^3 - 3\beta_v)d_{TA}^2c_{TA}^2, \quad (\text{S18})$$

$$d = (-\beta_v^9 + 6\beta_v^6 + 6\beta_v^4 - \beta_v)d_{TA}^3c_{TA}, \quad (\text{S19})$$

$$e = (2\beta_v^9 + 2\beta_v^4)d_{TA}^4. \quad (\text{S20})$$

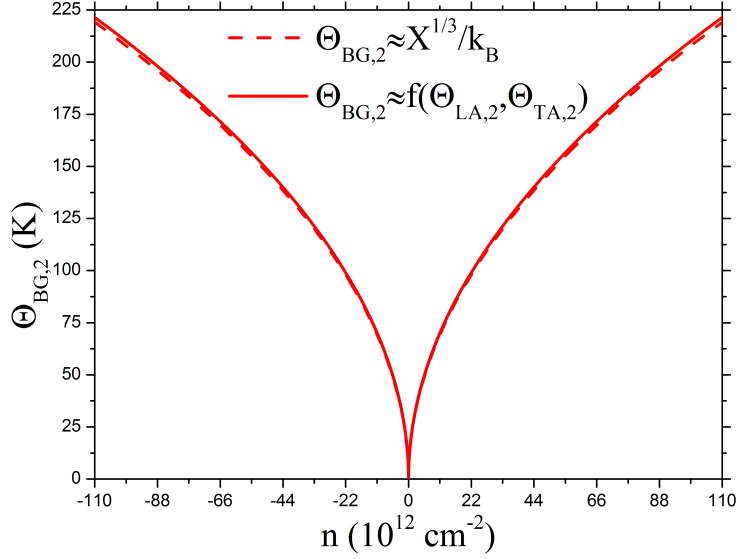


Figure S1. Doping-dependent Bloch-Grüneisen temperatures determined from $d^2\rho_\mu(\mu, T)/dT^2 = 0$. Dashed: exact solution given by Eq. (S21). Solid: approximated solution given by Eq. (S30) with $f(\Theta_{LA,2}, \Theta_{TA,2}) = \sqrt[3]{\frac{\Theta_{LA,2}^3 + \beta_v^2 \Theta_{TA,2}^3}{1 + \beta_v^2}}$.

Eliminate the complex (unphysical), negative, and zero roots, we obtain a single positive physical solution,

$$X = \frac{s + \sqrt{s^2 - 4(z_R + t)}}{2} - \frac{b}{4a}, \quad (\text{S21})$$

where

$$s = \sqrt{2z_R - p}, \quad (\text{S22})$$

$$t = -\sqrt{z_R^2 - r}, \quad (\text{S23})$$

$$z_R = \sqrt[3]{-\frac{Q}{2} + \sqrt{\frac{Q^2}{4} + \frac{P^3}{27}}} + \sqrt[3]{-\frac{Q}{2} - \sqrt{\frac{Q^2}{4} + \frac{P^3}{27}}} + \frac{p}{6}, \quad (\text{S24})$$

$$P = -r - \frac{p^2}{12}, \quad (\text{S25})$$

$$Q = -\frac{p^3}{108} + \frac{pr}{3} - \frac{q^2}{8}, \quad (\text{S26})$$

$$p = \frac{8ac - 3b^2}{8a^2}, \quad (\text{S27})$$

$$q = \frac{b^3 - 4abc + 8a^2d}{8a^3}, \quad (\text{S28})$$

$$r = \frac{16ab^2c - 64a^2bd + 256a^3e - 3b^4}{256a^4}. \quad (\text{S29})$$

Finally, we have

$$\Theta_{BG,2} \approx \frac{\sqrt[3]{X}}{k_B} \approx \sqrt[3]{\frac{\Theta_{LA,2}^3 + \beta_v^2 \Theta_{TA,2}^3}{1 + \beta_v^2}}, \quad (\text{S30})$$

where

$$k_B \Theta_{a,2} = \sqrt[3]{\frac{2d_a}{c_a}} = \sqrt[3]{\frac{16}{c_0}} \hbar v_a k_F \approx \hbar v_a k_F. \quad (\text{S31})$$

The way we obtain the approximated expression in Eq. (S30) is based on the following argument. In the limit $\beta_v = 1$, we should get $\sqrt[3]{X} = k_B \Theta_{a,2}$. Thus, X must take the form $\sqrt[3]{X} = k_B \sqrt[3]{\frac{\Theta_{LA,2}^3 + \alpha \Theta_{TA,2}^3}{1 + \alpha}}$. We also noticed that $\Theta_{BG,2} \approx 1.35 \Theta_{BG,1}$. Thus, X should be closer to the HT limit than LT limit, and in the HT limit we have $\alpha \rightarrow \beta_v^2$ as implied by Eq. (S5). In Fig. S1, we compare the exact solution given by Eq. (S21) and the approximated solution by Eq. (S30). It is found that the difference between the two is negligible.

-
- [1] J. M. Ziman, *Electrons and Phonons: The Theory of Transport Phenomena in Solids* (Oxford University Press, 1960).
 - [2] F. Bloch, *Zeitschrift fur Physik* 59, 208 (1930).
 - [3] E. Grüneisen, *Ann. Phys. (Leipzig)* 16, 530 (1933).
 - [4] M. S. Fuhrer, *Physics* 3, 106 (2010).
 - [5] V. K. Tewary and B. Yang, *PRB* 79, 125416 (2009).
 - [6] H. L. Stormer, L. N. Pfeiffer, K. W. Baldwin, and K. W. West, *Phys. Rev. B* 41, 1278 (1990).
 - [7] O. E. Raichev, A. T. Hatke, M. A. Zudov, and J. L. Reno, *Phys. Rev. B* 96, 081407(R) (2017).
 - [8] E. H. Hwang and S. D. Sarma, *Phys. Rev. B* 77, 115449 (2008).
 - [9] D. K. Efetov and P. Kim, *Phys. Rev. Lett.* 105, 256805 (2010).
 - [10] E. V. Castro, H. Ochoa, M. I. Katsnelson, R. Gorbachev, D. C. Elias, K. S. Novoselov, A. K. Geim, and F. Guinea, *Phys. Rev. Lett.* 105, 266601 (2010).
 - [11] T. Sohler, M. Calandra, C.-H. Park, N. Bonini, N. Marzari, and F. Mauri, *Phys. Rev. B* 90, 125414 (2014).
 - [12] C.-H. Park, N. Bonini, T. Sohler, G. Samsonidze, B. Kozinsky, M. Calandra, F. Mauri, and N. Marzari, *Nano Lett.* 14, 1113 (2014).
 - [13] Z. Li, J. Wang, and Z. Liu, *J. Chem. Phys.* 141, 144107 (2014).

- [14] P. Kumaravadivel, M. T. Greenaway, D. Perello, A. Berdyugin, J. Birkbeck, J. Wengraf, S. Liu, J. H. Edgar, A. K. Geim, L. Eaves, and R. K. Kumar, *Nat. Commun.* 10, 3334 (2019).
- [15] M. T. Greenaway, R. Krishna Kumar, P. Kumaravadivel, A. K. Geim, and L. Eaves, *Phys. Rev. B* 100, 155120 (2019).
- [16] K. V. Nguyen and Y. C. Chang, *Phys. Chem. Chem. Phys.* 22, 3999 (2020).
- [17] X. Cong, Q. Q. Li, X. Zhang, M. L. Lin, J. B. Wu, X. L. Liu, P. Venezuela, P. H. Tan, *Carbon* 149, 19 (2019).